Journal of NUCLEAR SCIENCE and TECHNOLOGY, Vol. 39, No. 10, p. 1015–1025 (October 2002)

Nonlinear Analytic and Semi-Analytic Nodal Methods for Multigroup Neutron Diffusion Calculations

Xue Dong FU and Nam Zin CHO*

Department of Nuclear and Quantum Engineering, Korea Advanced Institute of Science and Technology, 373-1 Kusong-dong, Yusong-gu, Taejon, Korea 305-701

(Received April 10, 2002 and accepted in revised form August 17, 2002)

Two advanced nodal methods for the solution of the multigroup neutron diffusion equations are developed, using the nonlinear coarse-mesh finite difference (CMFD) scheme. Based on the analytic and semi-analytic methods, the relationships between the flux and current on the nodal surface are derived, by which the two-node problem is formulated in an efficient way. The issue of the complex eigenmodes and the instability problem inherent in the analytic solution are considered in order to have an efficient and stable algorithm. The numerical results demonstrate the effectiveness of the two methods.

KEYWORDS: nonlinear nodal method, analytic method, semi-analytic method, two-node problem, complex eigenmodes, instability problem, neutron diffusion equation, multigroup theory, CMFD scheme

I. Introduction

The starting point of the modern nodal methods[1,2] is the nodal balance equation. The spatial coupling relationships are derived by applying higher-order approximations to the set of transverse-integrated diffusion equations coupled through transverse leakage terms. In the nonlinear iterative strategy,[3,4] the coarse-mesh finite difference (CMFD) equation is formed to represent the global coupling of a reactor core by assuming a simple finite-difference-like current equation

$$J_g = \frac{1}{h^L/D_g^L + h^R/D_g^R}(\bar{\phi}_g^L - \bar{\phi}_g^R) + DN_g(\bar{\phi}_g^L + \bar{\phi}_g^R), \tag{1}$$

where $\bar{\phi}_g$ and D_g are nodal average flux and diffusion coefficient in group g, h is the half width of the node. The superscripts L and R denote the left and right nodes. The coupling correction factor DN_g is determined by solving the two-node problem with the higher-order method and is updated in nonlinear iteration so that the calculation converges to the same result as that of the core-wise higher-order nodal method. Without compromising of accuracy, this nonlinear CMFD scheme can reduce the storage requirement and computing time associated with higher-order nodal methods.

The nodal methods presented in this paper employ this nonlinear scheme based on Eq. (1). In order to determine the coupling correction factor, the two-node problem should be formulated with the higher-order nodal scheme, in which the transverse-integrated diffusion equations are to be solved to obtain the interface current. Instead of solving such problem directly, we first derive the relationships between the flux and current on the nodal surface, based on the analytic and semi-analytic methods. The idea is based on the fact that in the problem each node serves as the boundary conditions for the other one. Under the necessary nodal constraints, the flux and current on the same nodal surface are not independent and their relationship can be worked out. In fact the derivation is straightforward when using the analytic method. Applications of the relationships to the two-node problem can lead to efficient solution methods, because we avoid solving the linear systems of higher order required in the conventional methods. Moreover, in the resulting analytic method, the problem with a near singular homogeneous solution turns into a removable one such that a more robust method is achieved.

In Chap. II, the equations relating the surface flux to current are first derived based on the two methods. The complex eigenmodes in the general multigroup analytic solution are considered. Then two-node solution methods are described and compared with the conventional methods. The numerical results for several benchmark problems are presented in Chap. III. Finally, conclusions are given in Chap. IV.

II. Theory and Method

1. Analytic Method

The analytic nodal method (ANM)[5] by Smith is characterized by the use of the analytic solution of the transverse-integrated diffusion equation in constructing the nodal scheme. Due to the algebraic complexity inherent in multigroup scheme, the ANM is normally restricted to two energy groups. In addition, the instability problem of the ANM solution with a near singular buckling matrix should be treated properly. We will apply the analytic solution of the multigroup transverse-integrated diffusion equation to the solution of the two-node problem.

(1) Structure of the Analytic Solution

We begin with the transverse-integrated diffusion equation written in matrix form

$$-\frac{d^2}{du^2}\phi(u) + \mathbf{A}\phi(u) = -\boldsymbol{l}(u), \tag{2}$$

where $\phi(u)$ is the column vector of the transverse-integrated flux with G elements (G is the number of energy groups), and $G\times G$ buckling matrix $\mathbf{A}$ is defined by

$$\mathbf{A} = \mathbf{D}^{-1}\left(\mathbf{S}_r - \mathbf{S}_s - \frac{1}{k_{\text{eff}}}\boldsymbol{\chi}\boldsymbol{\nu}\mathbf{S}_f\right).$$

*Corresponding author, Tel. +82-42-869-3819, Fax. +82-42-869-5859, E-mail: nzcho@mail.kaist.ac.kr

The transverse-leakage vector on the right-hand side of the equation has been premultiplied by $\mathbf{D}^{-1}$.

The analytic solution of Eq. (2) consists of homogeneous solution and one particular solution of the inhomogeneous equation. The homogeneous solution is dictated by the eigenvalues and eigenvectors of the matrix $\mathbf{A}$. For each eigenvalue λ_j and the corresponding eigenvector $\boldsymbol{r}_j$, there are two fundamental solution vectors $\boldsymbol{r}_j \cosh\sqrt{\lambda_j}u$ and $\boldsymbol{r}_j \sinh\sqrt{\lambda_j}u$. The homogeneous solution is the linear combination of $2G$ fundamental solution vectors. For general multigroup problems, it is possible that the eigenmode is complex-valued. Thus the formulation may involve complex arithmetic, which is undesirable as long as the efficiency is considered. To address the similar situation of the analytic function expansion nodal method (AFEN)[6] in treating complex eigenmodes, Cho *et al*. suggested a new transformation matrix by which the complex eigenmodes are transformed to real functions.[7] This rigorous algorithm has been successfully implemented in the AFEN method. Here we treat the problem by directly using equivalent real fundamental solution vectors that can be obtained from the complex ones. Because $\mathbf{A}$ is real, the complex eigenmodes must occur in conjugate pairs. Suppose λ_k and λ_k^* (The asterisk denotes complex conjugate.) are two complex eigenvalues of $\mathbf{A}$. By appropriate linear combination, four real solutions of the homogenous equation can be obtained:

$$\frac{1}{2}\left(\boldsymbol{r}_k \cosh\sqrt{\lambda_k}u + \boldsymbol{r}_k^* \cosh\sqrt{\lambda_k^*}u\right)$$
$$= \mathrm{Re}\,(\boldsymbol{r}_k)\cosh\alpha u\cos\beta u - \mathrm{Im}\,(\boldsymbol{r}_k)\sinh\alpha u\sin\beta u,$$

$$\frac{1}{2i}\left(\boldsymbol{r}_k \cosh\sqrt{\lambda_k}u - \boldsymbol{r}_k^* \cosh\sqrt{\lambda_k^*}u\right)$$
$$= \mathrm{Re}\,(\boldsymbol{r}_k)\sinh\alpha u\sin\beta u + \mathrm{Im}\,(\boldsymbol{r}_k)\cosh\alpha u\cos\beta u,$$

$$\frac{1}{2}\left(\boldsymbol{r}_k \sinh\sqrt{\lambda_k}u + \boldsymbol{r}_k^* \sinh\sqrt{\lambda_k^*}u\right)$$
$$= \mathrm{Re}\,(\boldsymbol{r}_k)\sinh\alpha u\cos\beta u - \mathrm{Im}\,(\boldsymbol{r}_k)\cosh\alpha u\sin\beta u,$$

$$\frac{1}{2i}\left(\boldsymbol{r}_k \sinh\sqrt{\lambda_k}u - \boldsymbol{r}_k^* \sinh\sqrt{\lambda_k^*}u\right)$$
$$= \mathrm{Re}\,(\boldsymbol{r}_k)\cosh\alpha u\sin\beta u + \mathrm{Im}\,(\boldsymbol{r}_k)\sinh\alpha u\cos\beta u,$$

where $\alpha+i\beta$ is one square root of λ_k. Since they are linearly independent, the four real vectors can be used as the fundamental solution vectors to replace the complex ones. By doing so, the two conjugate eigenmodes are actually combined with each other.

Let $\phi^p(u)$ be one particular solution and let matrix $\mathbf{R}$ have the eigenvectors as the columns, using $\mathrm{Re}(\boldsymbol{r}_k)$ and $\mathrm{Im}\,(\boldsymbol{r}_k)$ to replace the pair of conjugate eigenvectors. The analytic solution of Eq. (2) is

$$\phi(u) = \mathbf{R}(\mathbf{X}(u)\boldsymbol{c}_1 + \mathbf{Y}(u)\boldsymbol{c}_2) + \phi^p(u), \tag{3}$$

where $\boldsymbol{c}_1$, $\boldsymbol{c}_2$ are constant vectors, and $\mathbf{X}(u)$, $\mathbf{Y}(u)$ are block diagonal matrices defined by

$$\mathbf{X}_{jj}(u) = \begin{cases} \cosh\sqrt{\lambda_j}u, & \lambda_j > 0, \\ 1, & \lambda_j = 0, \\ \cos\sqrt{|\lambda_j|}u, & \lambda_j < 0, \\ \begin{pmatrix} \cosh\alpha u\cos\beta u & \sinh\alpha u\sin\beta u \\ -\sinh\alpha u\sin\beta u & \cosh\alpha u\cos\beta u \end{pmatrix}, & \lambda_j \text{ is complex}, \end{cases}$$

$$\mathbf{Y}_{jj}(u) = \begin{cases} \sinh\sqrt{\lambda_j}u, & \lambda_j > 0, \\ u, & \lambda_j = 0, \\ \sin\sqrt{|\lambda_j|}u, & \lambda_j < 0, \\ \begin{pmatrix} \sinh\alpha u\cos\beta u & \cosh\alpha u\sin\beta u \\ -\cosh\alpha u\sin\beta u & \sinh\alpha u\cos\beta u \end{pmatrix}, & \lambda_j \text{ is complex}. \end{cases}$$

In the above definitions, a real eigenvalue corresponds to a scalar function and a pair of complex eigenvalues corresponds to a 2×2 submatrix composed of real functions. Let n_j be the order of the j-th diagonal block, then $\sum_j n_j = G$.

(2) Particular Solution

To determine $\phi^p(u)$, it is advantageous to use transformation $\phi(u)=\mathbf{R}\xi(u)$ to reduce Eq. (2) to a decoupled form

$$-\frac{d^2}{du^2}\xi(u) + \mathbf{\Lambda}\xi(u) = -\hat{\boldsymbol{l}}(u), \tag{4}$$

where

$$\mathbf{\Lambda} = \mathbf{R}^{-1}\mathbf{A}\mathbf{R},$$
$$\hat{\boldsymbol{l}}(u) = \mathbf{R}^{-1}\boldsymbol{l}(u).$$

The block diagonal matrix $\mathbf{\Lambda}$ is given by

$$\mathbf{\Lambda}_{jj} = \begin{cases} \lambda_j, & \lambda_j \text{ is real}, \\ \begin{pmatrix} \mathrm{Re}\,(\lambda_j) & \mathrm{Im}\,(\lambda_j) \\ -\mathrm{Im}\,(\lambda_j) & \mathrm{Re}\,(\lambda_j) \end{pmatrix}, & \lambda_j \text{ is complex}. \end{cases} \tag{5}$$

Each eigenmode is separated from the others, except the complex ones that are coupled with each other in pairs.

The particular solution of Eq. (4) depends on the form of the inhomogeneous term as well as the eigenmode. The transverse leakage term is approximated by the quadratic fit that is common in the modern nodal methods. Therefore, the inhomogeneous term is quadratic

$$\hat{\boldsymbol{l}}(u) = \hat{\boldsymbol{l}}_0 + \hat{\boldsymbol{l}}_1 u + \hat{\boldsymbol{l}}_2\left(u^2 - \frac{1}{3}h^2\right), \tag{6}$$

where the basis functions are low order Legendre polynomials, h is the half width of the node. The solutions for zero and nonzero eigenmodes are of different forms, which will be discussed separately. For nonzero eigenmode, the particular solution is reasonably assumed to be quadratic

$$\xi_j(u) = \xi_{0j} + \xi_{1j}u + \xi_{2j}\left(u^2 - \frac{1}{3}h^2\right). \tag{7}$$

Inserting Eqs. (6) and (7) into Eq. (4) and equating the terms of the same order, we can obtain the equations for the expansion coefficients

$$\mathbf{\Lambda}_{jj}\xi_{0j} = -\hat{\boldsymbol{l}}_{0j} + 2\xi_{2j}, \tag{8a}$$

$$\mathbf{\Lambda}_{jj}\xi_{1j} = -\hat{\boldsymbol{l}}_{1j}, \tag{8b}$$

$$\mathbf{\Lambda}_{jj}\xi_{2j} = -\hat{\boldsymbol{l}}_{2j}. \tag{8c}$$

In the above equations, the splitting of $\xi(u)$ and $\hat{\boldsymbol{l}}(u)$ is consistent with that of $\mathbf{\Lambda}$.

When the eigenvalue is close to zero, the resulting expansion coefficients and therefore the particular solution may have very large magnitude. Although it is still a correct solution, very large numbers in the computation may lead to the instability problem due to the rounding errors, particularly in single-precision arithmetic. To overcome this problem, an approximation is made here by treating a near zero eigenmode as a zero eigenmode (for an alternate approach of the continued factoring method, see Ref. 8)). To find the particular solution for zero eigenmode, we use the more general method of variation of parameters. In the following discussion, we only consider a real eigenmode. Assume that the particular solution is similar in form to the homogenous solution but with unknown functions instead of unknown constants to be determined:

$$\xi_j(u) = c_1(u)\mathbf{X}_{jj}(u) + c_2(u)\mathbf{Y}_{jj}(u). \tag{9}$$

The unknown scalar functions $c_1(u)$ and $c_2(u)$ are required to satisfy

$$c_1'(u)\mathbf{X}_{jj}(u) + c_2'(u)\mathbf{Y}_{jj}(u) = 0,$$

$$c_1'(u)\mathbf{X}_{jj}'(u) + c_2'(u)\mathbf{Y}_{jj}'(u) = \hat{\boldsymbol{l}}_j(u),$$

where we use prime to denote differentiation. Solving the above two equations for $c_1'(u)$, $c_2'(u)$ and then integrating, we obtain

$$c_1(u) = -\frac{1}{\mu}\int^u \hat{\boldsymbol{l}}_j(v)\mathbf{Y}_{jj}(v)dv, \tag{10a}$$

$$c_2(u) = \frac{1}{\mu}\int^u \hat{\boldsymbol{l}}_j(v)\mathbf{X}_{jj}(v)dv, \tag{10b}$$

where

$$\mu = \begin{cases} \sqrt{|\lambda_j|}, & \lambda_j \neq 0, \\ 1, & \lambda_j = 0. \end{cases}$$

If integrating Eqs. (10) by parts, we can find that $c_1(u)$ and $c_2(u)$ may be functions having very large magnitude as the eigenvalue becomes close to zero. In this case, we let the eigenvalue be zero and use the linear functions to replace the trigonometric or hyperbolic functions as the eigenfunctions. Under this linear approximation, we have

$$c_1(u) = \left(-\frac{1}{2}\hat{\boldsymbol{l}}_{0j} + \frac{h^2}{6}\hat{\boldsymbol{l}}_{2j}\right)u^2 - \frac{1}{3}\hat{\boldsymbol{l}}_{1j}u^3 - \frac{1}{4}\hat{\boldsymbol{l}}_{2j}u^4 + b_1, \tag{11a}$$

$$c_2(u) = \left(\hat{\boldsymbol{l}}_{0j} - \frac{h^2}{3}\hat{\boldsymbol{l}}_{2j}\right)u + \frac{1}{2}\hat{\boldsymbol{l}}_{1j}u^2 + \frac{1}{3}\hat{\boldsymbol{l}}_{2j}u^3 + b_2. \tag{11b}$$

The integration constants in Eqs. (11) suggest that the particular solutions are not unique. Because any particular solution can be used, simply let b_1 and b_2 be zero. Accordingly, the particular solution for zero eigenmode is a fourth-order polynomial:

$$\xi_j(u) = \left(\frac{1}{2}\hat{\boldsymbol{l}}_{0j} - \frac{h^2}{6}\hat{\boldsymbol{l}}_{2j}\right)u^2 + \frac{1}{6}\hat{\boldsymbol{l}}_{1j}u^3 + \frac{1}{12}\hat{\boldsymbol{l}}_{2j}u^4. \tag{12}$$

Thus the particular solution of Eq. (4) is given by Eqs. (7) and (8) or alternatively by Eq. (12) in case of near zero eigenmode. $\phi^p(u)$ is then obtained through the transformation with the matrix $\mathbf{R}$.

When the buckling matrix $\mathbf{A}$ contains a zero eigenvalue, it is singular, meaning physically that in the node considered the production of neutrons in fission reactions balances the loss of neutrons due to absorptions and there is no net leakage out of the node. This happens when the infinite medium multiplication factor of the node equals the core effective multiplication factor. The instability problem with a near singular $\mathbf{A}$ is circumvented here by treating $\mathbf{A}$ as a singular matrix. A similar idea has been studied as a stabilization technique for nonlinear ANM,[9] although the discussion is limited to two-group case. The difference here lies in the treatment of the homogeneous solution. We will describe it in the following subsections. Because the eigenvalues of $\mathbf{A}$ need to be computed in the method, we identify a near singular case by directly observing the smallest real eigenvalue $|\lambda_j|_{\min}$. If the condition $|\lambda_j|_{\min} < \varepsilon$ is satisfied in a node, it is treated as a singular one and Eq. (12) is used instead to find the particular solution. The typical criterion used is $\varepsilon = 10^{-4}$.

(3) Relationship between Surface Flux and Current

The two unknown constant vectors in Eq. (3) are subject to the boundary conditions. If we know the nodal average flux, which is the case in the work, the even constant vector can be determine by the nodal average constraint

$$\bar{\phi} = \frac{1}{2h}\int_{-h}^{h}\phi(u)du = \mathbf{R}\bar{\mathbf{X}}c_1 + \bar{\phi}^p, \tag{13}$$

where $\bar{\mathbf{X}}$ and $\bar{\phi}^p$ are the averages of $\mathbf{X}(u)$ and $\phi^p(u)$ over the nodal width. So $\boldsymbol{c}_1$ can be written as

$$\boldsymbol{c}_1 = (\mathbf{R}\bar{\mathbf{X}})^{-1}(\bar{\phi} - \bar{\phi}^p). \tag{14}$$

The odd constant vector cannot be determined without the boundary condition. Since Eq. (3) has only G degrees of freedom, the flux and current on the same nodal surface cannot be specified arbitrarily. In fact they are dependent on each other and we want to derive the relationship between them. According to Eq. (3), the flux and current on the positive or negative

nodal surfaces can be expressed as

$$\phi_\pm = \phi(\pm h) = \mathbf{R}(\mathbf{X}\boldsymbol{c}_1 \pm \mathbf{Y}\boldsymbol{c}_2) + \phi_\pm^p, \tag{15}$$

$$\boldsymbol{J}_\pm = -\mathbf{D}\frac{d}{du}\phi(u)\Big|_{u=\pm h} = -\mathbf{DR}(\pm\hat{\mathbf{X}}\boldsymbol{c}_1 + \hat{\mathbf{Y}}\boldsymbol{c}_2) + \boldsymbol{J}_\pm^p, \tag{16}$$

where matrices $\mathbf{X}$ and $\hat{\mathbf{X}}$ are obtained respectively by evaluating $\mathbf{X}(u)$ and its first derivative at $u=h$, $\mathbf{Y}$ and $\hat{\mathbf{Y}}$ are defined in an analogous manner. The definitions of $\phi_\pm^p$ and $\boldsymbol{J}_\pm^p$ manifest themselves in the equations. We insert Eq. (14) into Eqs. (15) and (16) written for each surface and then eliminate $\boldsymbol{c}_2$ in favor of the current on that surface. The resulting equations for both surfaces can be collectively written as

$$\phi_\pm = \mp\mathbf{C}(\boldsymbol{J}_\pm - \hat{\boldsymbol{J}}_\pm) + \hat{\phi}_\pm, \tag{17}$$

where

$$\mathbf{C} = \mathbf{R}(\mathbf{Y}\hat{\mathbf{Y}}^{-1})\mathbf{R}^{-1}\mathbf{D}^{-1}, \tag{18}$$

$$\hat{\phi}_\pm = \mathbf{R}(\mathbf{X}\bar{\mathbf{X}}^{-1})\hat{\boldsymbol{c}}_1 + \phi_\pm^p, \tag{19}$$

$$\hat{\boldsymbol{J}}_\pm = \mp\mathbf{DR}(\hat{\mathbf{X}}\bar{\mathbf{X}}^{-1})\hat{\boldsymbol{c}}_1 + \boldsymbol{J}_\pm^p, \tag{20}$$

$$\hat{\boldsymbol{c}}_1 = \mathbf{R}^{-1}(\bar{\phi} - \bar{\phi}^p). \tag{21}$$

$\mathbf{X}\bar{\mathbf{X}}^{-1}$, $\hat{\mathbf{X}}\bar{\mathbf{X}}^{-1}$ and $\mathbf{Y}\hat{\mathbf{Y}}^{-1}$ have the same structure as $\mathbf{X}$ or $\mathbf{Y}$ and can be predetermined as

$$(\mathbf{X}\bar{\mathbf{X}}^{-1})_{jj} = \begin{cases} \dfrac{\sqrt{\lambda_j}h}{\tanh\sqrt{\lambda_j}h}, & \lambda_j > 0, \\ 1, & \lambda_j = 0, \\ \dfrac{\sqrt{|\lambda_j|}h}{\tan\sqrt{|\lambda_j|}h}, & \lambda_j < 0, \\ c_X \begin{pmatrix} \alpha\gamma + \beta\sigma & -\alpha\sigma + \beta\gamma \\ \alpha\sigma - \beta\gamma & \alpha\gamma + \beta\sigma \end{pmatrix}, & \lambda_j \text{ is complex}, \end{cases} \tag{22}$$

$$(\hat{\mathbf{X}}\bar{\mathbf{X}}^{-1})_{jj} = h\boldsymbol{\Lambda}_{jj}, \tag{23}$$

$$(\mathbf{Y}\hat{\mathbf{Y}}^{-1})_{jj} = \begin{cases} \dfrac{\tanh\sqrt{\lambda_j}h}{\sqrt{\lambda_j}}, & \lambda_j > 0, \\ h, & \lambda_j = 0, \\ \dfrac{\tan\sqrt{|\lambda_j|}h}{\sqrt{|\lambda_j|}}, & \lambda_j < 0, \\ c_Y \begin{pmatrix} \alpha\gamma + \beta\sigma & \alpha\sigma - \beta\gamma \\ -\alpha\sigma + \beta\gamma & \alpha\gamma + \beta\sigma \end{pmatrix}, & \lambda_j \text{ is complex}, \end{cases} \tag{24}$$

where

$$\gamma = \cosh\alpha h \sinh\alpha h,$$

$$\sigma = \cos\beta h \sin\beta h,$$

$$c_X = \frac{h}{(\sinh\alpha h\cos\beta h)^2 + (\cosh\alpha h\sin\beta h)^2},$$

$$c_Y = \frac{1}{(\alpha^2+\beta^2)[(\cosh\alpha h\cos\beta h)^2 + (\sinh\alpha h\sin\beta h)^2]}.$$

$\boldsymbol{\Lambda}_{jj}$ is defined by Eq. (5). According to the definitions, $(\mathbf{X}\bar{\mathbf{X}}^{-1})_{jj}$ and $(\mathbf{Y}\hat{\mathbf{Y}}^{-1})_{jj}$ are continuous at $\lambda_j{=}0$. As $\lambda_j{\to}0$, the limits are indeterminate form of the type $0/0$. Such singularities are removable and from numerical point of view the algorithms are very stable. No approximation is needed in case of a near singular $\mathbf{A}$. Therefore the stability consideration is only confined to the particular solution. As will be mentioned, this brings one advantage over the conventional method.

In defining Eq. (17), only $\mathbf{R}$ is a full matrix and one full matrix inverse needs to be computed. If the eigenvalues and eigenvectors of $\mathbf{A}$ are known, the algorithm is very efficient. For two-group calculations, the 2×2 matrix eigenproblem can be solved without any difficulty, whereas for general multigroup calculations, a sophisticated similarity transformation is required to solve the matrix eigenproblem.

2. Semi-Analytic Method

The general idea of semi-analytic method dates back to the work by Shober[10] for fast-reactor calculations and the more recent work by Wagner[11] and by Rajic and Ougouag.[12] While the ANM makes use of the analytic solution of the transverse-integrated diffusion equation, like the case in the nodal Green's function method (NGFM),[13] the analytic procedure in the semi-analytic method is based on the within-group equation and a quadratic effective source profile. Unlike the ANM in which the only approximation is the quadratic representation of the transverse leakage terms, additional approximations are introduced into the shape of the group source terms. Because the semi-analytic method avoids the algebraic complexity, it can be readily extended to multigroup problems.

(1) Semi-Analytic Solution and Constraint Equations

We rewrite Eq. (2) in a familiar form

$$-\frac{d^2}{du^2}\phi(u)+\hat{\mathbf{S}}\phi(u)=\mathbf{M}\phi(u)-\boldsymbol{l}(u), \tag{25}$$

where

$$\hat{\mathbf{S}}=\mathbf{D}^{-1}\mathbf{S}_r,$$

$$\mathbf{M}=\mathbf{D}^{-1}\left(\mathbf{S}_s+\frac{1}{k_{\text{eff}}}\boldsymbol{\chi}\boldsymbol{\nu}\mathbf{S}_f\right).$$

Provided that the group source terms and the transverse-leakage terms are projected onto quadratic Legendre polynomials, the analytic solution can be written as

$$\phi(u)=\boldsymbol{a}_0+u\boldsymbol{a}_1+\left(u^2-\frac{1}{3}h^2\right)\boldsymbol{a}_2+\left(\sinh\sqrt{\hat{\mathbf{S}}}u\right)\boldsymbol{a}_3+\left(\cosh\sqrt{\hat{\mathbf{S}}}u\right)\boldsymbol{a}_4, \tag{26}$$

where matrix functions are used, and $\boldsymbol{a}_m$'s are constant vectors to be determined. Since $\hat{\mathbf{S}}$ is a diagonal matrix, the two hyperbolic matrix functions are also diagonal matrices. The solution is required to satisfy the nodal average flux constraint

$$\boldsymbol{a}_0+\mathbf{B}_0\boldsymbol{a}_4=\bar{\phi}, \tag{27}$$

and the following moment equations up to the second order, which are obtained by applying a weighted residual procedure to Eq. (25) using Legendre polynomials as weight functions,

$$\hat{\mathbf{S}}\boldsymbol{a}_0-2\boldsymbol{a}_2=\mathbf{M}\bar{\phi}-\boldsymbol{l}_0, \tag{28}$$

$$\mathbf{A}\boldsymbol{a}_1=\mathbf{M}\mathbf{B}_1\boldsymbol{a}_3-\boldsymbol{l}_1, \tag{29}$$

$$\mathbf{A}\boldsymbol{a}_2=\mathbf{M}\mathbf{B}_2\boldsymbol{a}_4-\boldsymbol{l}_2, \tag{30}$$

where $\boldsymbol{l}_n$'s are low order Legendre expansion coefficients of $\boldsymbol{l}(u)$, and $\mathbf{B}_n$'s are given by

$$\mathbf{B}_0=\frac{1}{\langle 1,\ 1\rangle}\left\langle 1,\ \cosh\sqrt{\hat{\mathbf{S}}}u\right\rangle,$$

$$\mathbf{B}_1=\frac{1}{\langle u,\ u\rangle}\left\langle u,\ \sinh\sqrt{\hat{\mathbf{S}}}u\right\rangle,$$

$$\mathbf{B}_2=\frac{1}{\left\langle u^2-\frac{1}{3}h^2,\ u^2-\frac{1}{3}h^2\right\rangle}\left\langle u^2-\frac{1}{3}h^2,\ \cosh\sqrt{\hat{\mathbf{S}}}u\right\rangle,$$

and the inner product is defined as

$$\langle f_1(u),\ f_2(u)\rangle=\int_{-h}^{h}f_1(u)\,f_2(u)du.$$

In deriving Eqs. (28), (29) and (30), we have used Eq. (27) and the relationship $\mathbf{A}=\hat{\mathbf{S}}-\mathbf{M}$. Equations (28), (29) and (30) are the moment equations, *i.e.*, the weak form equations of Eq. (25). In other words, such determined solution should satisfy Eq. (25) in an integral sense. Because the model contains the transcendental components, it is expected to be more accurate than the fourth-order polynomial model as is used in the nodal expansion method (NEM).[14)]

(2) Relationship between Surface Flux and Current

Note that the even constant vectors can be solved in each node. Using Eqs. (27) and (28), $\boldsymbol{a}_0$ and $\boldsymbol{a}_2$ are expressed in terms of $\boldsymbol{a}_4$:

$$\boldsymbol{a}_0=\bar{\phi}-\mathbf{B}_0\boldsymbol{a}_4, \tag{31}$$

$$\boldsymbol{a}_2=\frac{1}{2}(\mathbf{A}\bar{\phi}+\boldsymbol{l}_0-\hat{\mathbf{S}}\mathbf{B}_0\boldsymbol{a}_4). \tag{32}$$

By inserting Eq. (32) into Eq. (30), the equation for solving $\boldsymbol{a}_4$ is

$$(\mathbf{A}\hat{\mathbf{S}}\mathbf{B}_0+2\mathbf{M}\mathbf{B}_2)\boldsymbol{a}_4=\mathbf{A}(\mathbf{A}\bar{\phi}+\boldsymbol{l}_0)+2\boldsymbol{l}_2. \tag{33}$$

$\boldsymbol{a}_0$ and $\boldsymbol{a}_2$ can be computed from Eqs. (31) and (32) by back substitution of $\boldsymbol{a}_4$. Then using Eq. (26), the flux and current on the positive or negative nodal surfaces are expressed in terms of the odd constant vectors and $\boldsymbol{a}_1$ and $\boldsymbol{a}_3$

$$\phi_\pm=\pm h\boldsymbol{a}_1\pm\left(\sinh\sqrt{\hat{\mathbf{S}}}h\right)\boldsymbol{a}_3+\boldsymbol{e}_\phi, \tag{34}$$

$$\boldsymbol{J}_\pm=-\mathbf{D}\left[\boldsymbol{a}_1+\left(\sqrt{\hat{\mathbf{S}}}\cosh\sqrt{\hat{\mathbf{S}}}h\right)\boldsymbol{a}_3\right]\pm\boldsymbol{e}_J, \tag{35}$$

where

$$\boldsymbol{e}_\phi=\boldsymbol{a}_0+\frac{2}{3}h^2\boldsymbol{a}_2+\left(\cosh\sqrt{\hat{\mathbf{S}}}h\right)\boldsymbol{a}_4, \tag{36}$$

$$\boldsymbol{e}_J=-\mathbf{D}\left[2h\boldsymbol{a}_2+\left(\sqrt{\hat{\mathbf{S}}}\sinh\sqrt{\hat{\mathbf{S}}}h\right)\boldsymbol{a}_4\right]. \tag{37}$$

Now the two unknown odd constant vectors provide Eqs. (34) and (35) with $2G$ degrees of freedom. By using the moment equation (29), we eliminate either $\boldsymbol{a}_1$ or $\boldsymbol{a}_3$ in the equations. Then there are only G degrees of freedom left. The similar idea as that applied in the analytic method can be used to derive the relationship between the flux and surface on the same nodal surface. In the derivation, Eq. (29) must be used with care. Note that the following two equations,

$$\boldsymbol{a}_1=\mathbf{A}^{-1}(\mathbf{M}\mathbf{B}_1\boldsymbol{a}_3-\boldsymbol{l}_1) \tag{38}$$

and

$$\boldsymbol{a}_3=(\mathbf{M}\mathbf{B}_1)^{-1}(\mathbf{A}\boldsymbol{a}_1+\boldsymbol{l}_1) \tag{39}$$

can be derived from Eq. (29). If the inverses of both $\mathbf{A}$ and $\mathbf{M}$ exist, the two equations are equivalent. However, Eq. (38) can be ill-conditioned when $\mathbf{A}$ is near singular. On the other hand, $\mathbf{M}$ is singular for non-fuel material. Because the two matrices cannot be singular or near singular at the same time, in case of near singular $\mathbf{A}$, we use Eq. (39), otherwise we use Eq. (38). As matrix $\mathbf{A}$ becomes near singular, the norm of $\mathbf{A}^{-1}$ becomes very large. Thus this norm can be a measure of the degree of near singularity, and if it is greater than a certain specified value $\mathbf{A}$ is considered to be near singular. In this paper we use row-sum norm and a criterion $\|\mathbf{A}^{-1}\|_\infty>10^4$ to identify a near-singular case. Unlike the instability problem encountered in the analytic method, no approximation is made here in order to have a stable algorithm. The final equations for both surfaces can be cast into the same form as Eq. (17):

$$\phi_\pm=\mp\mathbf{C}(\boldsymbol{J}_\pm-\hat{\boldsymbol{J}}_\pm)+\hat{\phi}_\pm, \tag{40}$$

where two sets of $\mathbf{C}$, $\hat{\phi}_\pm$ and $\hat{\boldsymbol{J}}_\pm$ can be obtained. Using Eq. (38), we have

$$\mathbf{C}=\left(h\hat{\mathbf{A}}+\sinh\sqrt{\hat{\mathbf{S}}}h\right)\left(\hat{\mathbf{A}}+\sqrt{\hat{\mathbf{S}}}\cosh\sqrt{\hat{\mathbf{S}}}h\right)^{-1}\mathbf{D}^{-1}, \tag{41}$$

$$\hat{\phi}_{\pm} = \mp h\hat{\mathbf{l}}_1 + \boldsymbol{e}_{\phi}, \tag{42}$$

$$\hat{\boldsymbol{J}}_{\pm} = \mathbf{D}\hat{\mathbf{l}}_1 \pm \boldsymbol{e}_J, \tag{43}$$

where

$$\hat{\mathbf{A}} = \mathbf{A}^{-1}\mathbf{M}\mathbf{B}_1,$$

$$\hat{\boldsymbol{l}}_1 = \mathbf{A}^{-1}\boldsymbol{l}_1.$$

Using Eq. (39), we have

$$\mathbf{C} = \left[h\mathbf{I} + \left(\sinh\sqrt{\hat{\mathbf{S}}}h\right)\tilde{\mathbf{A}}\right] \times \left[\mathbf{I} + \left(\sqrt{\hat{\mathbf{S}}}\cosh\sqrt{\hat{\mathbf{S}}}h\right)\tilde{\mathbf{A}}\right]^{-1}\mathbf{D}^{-1}, \tag{44}$$

$$\hat{\phi}_{\pm} = \pm\left(\sinh\sqrt{\hat{\mathbf{S}}}h\right)\tilde{\boldsymbol{l}}_1 + \boldsymbol{e}_{\phi}, \tag{45}$$

$$\hat{\boldsymbol{J}}_{\pm} = -\mathbf{D}\left(\sqrt{\hat{\mathbf{S}}}\cosh\sqrt{\hat{\mathbf{S}}}h\right)\tilde{\boldsymbol{l}}_1 \pm \boldsymbol{e}_J, \tag{46}$$

where

$$\tilde{\mathbf{A}} = (\mathbf{M}\mathbf{B}_1)^{-1}\mathbf{A},$$

$$\tilde{\boldsymbol{l}}_1 = (\mathbf{M}\mathbf{B}_1)^{-1}\boldsymbol{l}_1.$$

In Eq. (44), $\mathbf{I}$ is a $G\times G$ identity matrix. It is found that if the inverses of both $\mathbf{A}$ and $\mathbf{M}$ exist, Eqs. (41) and (44) give the same result. When $\mathbf{A}$ is near singular, Eqs. (44), (45) and (46) will be used alternatively so that the algorithm keeps stable. Note that only $\mathbf{A}$ and $\mathbf{M}$ are full matrices. To obtain Eq. (40), three full matrix inverses need to be computed and each inverse problem is of order G.

3. Transverse-Leakage Approximation

So far we have applied the analytic and semi-analytic solutions of the transverse-integrated diffusion equation with quadratic transverse-leakage profile. In the work, the expansion coefficients of the leakage term are determined so as to preserve the average transverse leakage in the three consecutive nodes. This technique was developed on a somewhat ad hoc basis, however, it has been widely used in most transverse-integrated nodal methods.[2] One study revealed that although this quadratic leakage fit is usually quite good, there are cases where large errors in the leakage shape can be produced.[5] This is one of the prime limitations of the transverse integration procedure. Since the transverse-leakage approximation is the only approximation made in the analytic method, all of the resulting errors in the calculations must be due to the inaccurate representation of the transverse-leakage profile.

4. Two-Node Solution Methods

In order to update the coupling correction factor, the two-node problem is to be solved during the nonlinear iteration. Provided that the nodal average flux, transverse leakage and effective multiplication factor are known from the most recent iterative solution of the CMFD equation, Eq. (17) or (40) can be obtained for each node surface. In a two-node problem, the equations for the positive surface of the left node are related to the equations for the negative surface of the right node by imposing the following continuity conditions:

$$\mathbf{F}_+^L\phi_+^L = \mathbf{F}_-^R\phi_-^R, \tag{47}$$

$$\boldsymbol{J}_+^L = \boldsymbol{J}_-^R, \tag{48}$$

where $\mathbf{F}$ is a diagonal matrix consisting of the discontinuity factors. By eliminating the surface fluxes in the equations, we obtain a $G\times G$ equation for the interface current

$$(\mathbf{F}_-^R\mathbf{C}^R + \mathbf{F}_+^L\mathbf{C}^L)\boldsymbol{J}_+^L = \mathbf{F}_-^R(\mathbf{C}^R\hat{\boldsymbol{J}}_-^R - \hat{\phi}_-^R) + \mathbf{F}_+^L(\mathbf{C}^L\hat{\boldsymbol{J}}_+^L + \hat{\phi}_+^L). \tag{49}$$

After the interface current is solved, the coupling correction factor is determined such that the current given by Eq. (1) can match the solution of the two-node problem.

In the conventional methods, the basic idea is to first solve the unknown constants of the transverse-integrated flux in a two-node problem. Then the interface current is calculated by using a Fick's law. As we have seen, the even constants of each node can be determined without considering the continuity conditions. But the odd constants of the two coupling nodes are dependent on each other and must be solved simultaneously. The constraint equations for odd constants include the continuity conditions and the moment equations if necessary. By using Eqs. (15) and (16) and the continuity conditions, a $2G\times 2G$ equation for the odd constant vectors in the analytic solutions can be written as

$$\begin{pmatrix} (\mathbf{F}_+\mathbf{R}\mathbf{Y})^L & (\mathbf{F}_-\mathbf{R}\mathbf{Y})^R \\ -(\mathbf{D}\mathbf{R}\hat{\mathbf{Y}})^L & (\mathbf{D}\mathbf{R}\hat{\mathbf{Y}})^R \end{pmatrix}\begin{pmatrix} \boldsymbol{c}_2^L \\ \boldsymbol{c}_2^R \end{pmatrix} = \begin{pmatrix} \mathbf{F}_-^R(\mathbf{R}\mathbf{X}\boldsymbol{c}_1 + \phi_-^p)^R - \mathbf{F}_+^L(\mathbf{R}\mathbf{X}\boldsymbol{c}_1 + \phi_+^p)^L \\ (\mathbf{D}\mathbf{R}\hat{\mathbf{X}}\boldsymbol{c}_1 + \boldsymbol{J}_-^p)^R + (\mathbf{D}\mathbf{R}\hat{\mathbf{X}}\boldsymbol{c}_1 - \boldsymbol{J}_+^p)^L \end{pmatrix}, \tag{50}$$

where the even constant vectors $\boldsymbol{c}_1$ is solved by using Eq. (14). In the semi-analytic solution, there are two odd constant vectors to be determined for each node, namely $\boldsymbol{a}_1$ and $\boldsymbol{a}_3$. In addition to the continuity conditions, the moment equation (29) is also needed. The final $4G\times 4G$ equation for the odd constant vectors is

$$\begin{pmatrix} \mathbf{A}^L & -(\mathbf{M}\mathbf{B}_1)^L & \mathbf{0} & \mathbf{0} \\ (h\mathbf{F}_+)^L & \left(\mathbf{F}_+\sinh\sqrt{\hat{\mathbf{S}}}h\right)^L & (h\mathbf{F}_-)^R & \left(\mathbf{F}_-\sinh\sqrt{\hat{\mathbf{S}}}h\right)^R \\ -\mathbf{D}^L & -\left(\mathbf{D}\sqrt{\hat{\mathbf{S}}}\cosh\sqrt{\hat{\mathbf{S}}}h\right)^L & \mathbf{D}^R & \left(\mathbf{D}\sqrt{\hat{\mathbf{S}}}\cosh\sqrt{\hat{\mathbf{S}}}h\right)^R \\ \mathbf{0} & \mathbf{0} & \mathbf{A}^R & -(\mathbf{M}\mathbf{B}_1)^R \end{pmatrix}\begin{pmatrix} \boldsymbol{a}_1^L \\ \boldsymbol{a}_3^L \\ \boldsymbol{a}_1^R \\ \boldsymbol{a}_3^R \end{pmatrix} = \begin{pmatrix} -\boldsymbol{l}_1^L \\ (\mathbf{F}_-\boldsymbol{e}_{\phi})^R - (\mathbf{F}_+\boldsymbol{e}_{\phi})^L \\ -\boldsymbol{e}_J^R - \boldsymbol{e}_J^L \\ -\boldsymbol{l}_1^R \end{pmatrix}, \tag{51}$$

where the vectors $\boldsymbol{e}_{\phi}$ and $\boldsymbol{e}_J$ are given by Eqs. (36) and (37). The even constant vectors involved are determined by using

Eqs. (31), (32) and (33).

The orders of the linear systems defined by Eqs. (50) and (51) are $2G$ and $4G$, however, by using Eq. (49) the orders of the problems to be solved reduce to G. Numerical comparisons with the conventional methods show that the proposed methods are of the same accuracies but reduce the CPU times for the two-node calculations. For two-group problems, about 20% and 30% savings in CPU times are achieved, respectively, by the proposed analytic and semi-analytic methods. For four-group problems, the above savings are about 26% and 40%. Another advantage is associated with the stabilization technique for the analytic method. Note that $\mathbf{Y}$ and $\hat{\mathbf{Y}}$ in Eq. (50) are block diagonal matrices. When the buckling matrix $\mathbf{A}$ has an eigenvalue close to zero, the corresponding diagonal elements approach zero, which will cause a column of the $2G \times 2G$ matrix in Eq. (50) to approach a zero vector. Therefore Eq. (50) can be ill-conditioned if any one of the two nodes is near singular. This is another source of the instability problem besides the one from the particular solution. To avoid the ill-conditioning problem, linear approximation to the homogeneous solution can be adopted,[9] in which the linear functions are used to replace the trigonometric or hyperbolic functions as the eigenfunctions. Equivalent approximation in the proposed method is the use of zero eigenvalue when evaluating $(\mathbf{X}\bar{\mathbf{X}}^{-1})_{jj}$, $(\hat{\mathbf{X}}\bar{\mathbf{X}}^{-1})_{jj}$ and $(\mathbf{Y}\hat{\mathbf{Y}}^{-1})_{jj}$ with Eqs. (22), (23) and (24), respectively. But it is not necessary here because the singularities encountered are removable and no ill-conditioning problem happens. More importantly, the linear approximation to the homogeneous solution is likely to become worse as the degree of near singularity decreases. It is advantageous to avoid this approximation. In the next chapter, we will demonstrate this in a numerical example.

III. Results and Discussion

The proposed methods have been implemented into the nodal methods by using the nonlinear CMFD scheme. In the methods, the CMFD equation is solved by the fission source iteration procedure, using Wielandt's method to accelerate the outer iteration. SOR method is used in the inner iteration to invert the flux coefficient matrix. In the analytic nodal method, an implicitly double-shifted QR algorithm[15] is used to compute the eigenvalues and eigenvectors of the buckling matrix in multigroup option. In this chapter, we present results for several two-group light water reactor benchmark problems and for two four-group problems. Except where noted, all calculations were done using an assembly-size mesh and quarter-core planar symmetry. A convergence criterion of 10^{-5} for the node-wise fission source was used in the calculations. The CPU times are for the SUN-ULTRA1 workstation.

1. OECD-L336 (C5) Benchmark Problem

The OECD-L336 problem[16] was issued by the OECD-NEA Nuclear Science Committee to test the applicability of various modern core analysis methods to a core loaded with mixed-oxide (MOX) fuel assemblies. The C5 configuration that we used consists of two types of fuel assemblies (*i.e.*, uranium oxide (UO_2) and MOX fuel assemblies) and water reflector. Each fuel assembly is 21.42 cm wide and contains 17×17 homogenized pin cells of different types. The problem is characterized by the presence of large thermal flux gradients near the interfaces between the UO_2 and MOX fuel assemblies, because of very different neutronic properties of the two types of fuel assemblies. For this problem, it was shown in Ref. 6) that the fourth-order polynomial scheme of NEM fails to predict the large flux variations accurately near the assembly interface, and the maximum error of nodal average thermal flux obtained by using NEM can be as high as 3.6%. **Table 1** gives the results of our calculations. Compared to heterogeneous VENTURE[17] finite-difference solution, the maximum errors in the assembly power density are only 0.59% and 1.17%, respectively, for the analytic and semi-analytic calculations. The analytic result is appreciably more accurate than semi-analytic result. This indicates that the analytic method is superior to the semi-analytic method in modeling the local steep thermal flux gradients due to strong discontinuity of the materials. The computer times here are too short to be used for a comparison.

2. Two-Dimensional IAEA Benchmark Problem

The two-dimensional IAEA benchmark problem[18] is a two-group model of a pressurized water reactor (PWR), which has been widely used to test the performance of the nodal schemes. The two-zone core consists of 177 homogenized fuel assemblies, each with a width of 20 cm. The core is reflected radially by 20 cm thick water. **Table 2** summarizes the results for this problem. The reference solution is the VENTURE finite-difference extrapolated solution published in Ref. 18). Using the assembly-size mesh, both the analytic and semi-analytic calculations are quite accurate: the maximum errors in the assembly power densities are less than 1%. The semi-analytic results are somewhat more accurate than the analytic results, however, the analytic calculations are faster than the semi-analytic calculations. Due to the inaccurate representation of transverse leakage profile by the quadratic fit, the transverse-integrated equation is only an approximate model. The associated error can be large, particularly when too coarse a mesh is used. This may explain the reason why in some cases more rigorous solution method to an approximate model does not necessarily give better results.

3. Ulchin-1 Cycle 1 Problem

This two-group two-dimensional PWR problem is based on Ulchin unit 1 core at the beginning of cycle one.[6] The core is a Framatome-type PWR rated at 2,775 MW (thermal),

Table 1 Comparison of results for the OECD-L336 (C5) benchmark problem

Method	k_{eff}	E_{max} [a] (%)	E_{rms} [b] (%)	CPU (s)
Analytic method	0.938377	0.59	0.30	0.01
Semi-analytic method	0.937612	1.17	0.73	0.01
Reference	0.937915			

[a] Maximum error in assembly average power densities

[b] Root mean square error in assembly average power densities

Table 2 Summary of results for the two-dimensional IAEA benchmark problem

Method	Meshes/Assembly	k_{eff} [a)]	$E_{\max}$ (%)	E_{rms} (%)	CPU (s)
Analytic method	1×1	1.029666	0.88	0.29	0.08
Semi-analytic method		1.029609	0.46	0.24	0.09
Analytic method	2×2	1.029606	0.32	0.12	0.28
Semi-analytic method		1.029603	0.28	0.10	0.33

a) Reference: 1.029585

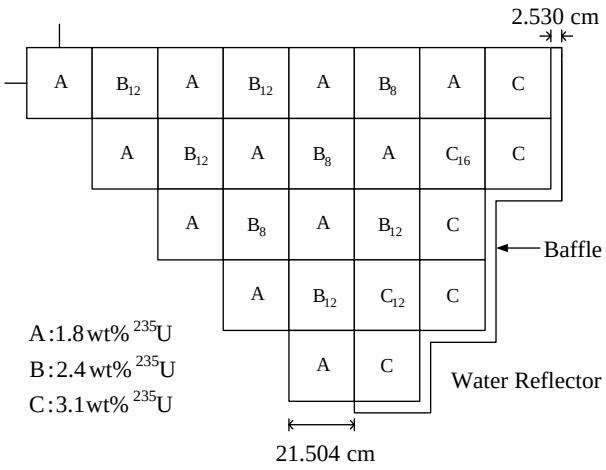

Fig. 1 The octant configuration of Ulchin-1 core at cycle 1
The figires written as a subscript denote the number of bundle absorber rods.

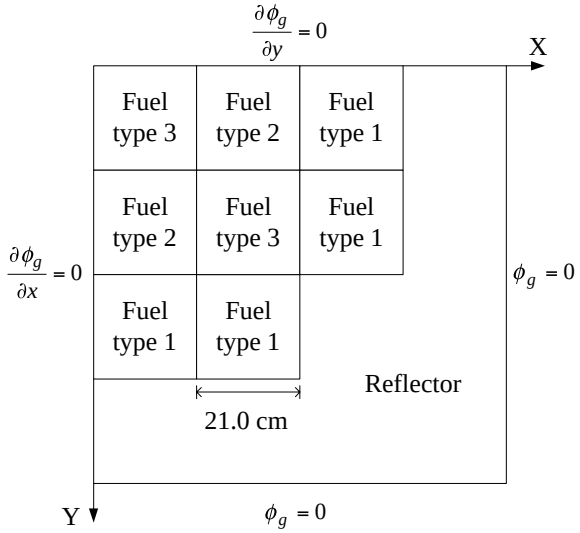

Fig. 2 The configuration of four-group MOX-fueled core problem

Table 3 Comparison of results for the Ulchin-1 cycle 1 problem

Method	k_{eff}	$E_{\max}$ (%)	E_{rms} (%)	CPU (s)
Analytic method	1.00109	1.29	0.73	0.09
Semi-analytic method	1.00104	1.05	0.56	0.11
Reference	1.00130			

which consists of 157 fuel assemblies. Each fuel assembly is 21.504 cm wide and contains 17×17 pin cells of different types. **Figure 1** illustrates the fuel loading pattern in octant core configuration. The complete problem and the homogenization procedure used were described in Ref. 6). The reference solution was obtained from heterogeneous VENTURE fine-mesh calculation. As is shown in **Table 3**, the two methods give comparable results, with the semi-analytic result a little more accurate. Again, the analytic calculation is faster than the semi-analytic calculation. This can be justified in view of the highly efficient procedure for solving 2×2 matrix eigenproblems in two-group calculations and the fact that the analytic method requires apparently less operations on vectors and matrices than the semi-analytic method.

4. Four-Group MOX-Fueled Core Problem

To demonstrate their multigroup capabilities, the two nodal methods were also applied to two four-group problems, one of which is a two-dimensional MOX-fueled core problem defined in Ref. 19). Shown in **Fig. 2**, the core consists of three types of homogenized fuel assemblies including MOX fuel assemblies. Each assembly is 21 cm wide. The reference solution was obtained from the analytic nodal calculation using 3.5 cm mesh (36 meshes per assembly). **Table 4** shows that accurate results can be obtained even when the assembly-size mesh is used. The analytic nodal results are slightly more accurate than the semi-analytic results. It appears not so hard to obtain the accurate result for this problem. In fact, the primary motivation for developing this problem was to test the new algorithm of the AFEN method to deal with the complex eigenmodes for extension to multigroup problem. Since the analytic nodal calculations here are accurate, the method developed to avoid complex arithmetic is correct and effective. The results (also the results of the KOEBERG problem below) indicate that the analytic nodal calculations require about 30% more CPU time than the semi-analytic calculations. This is because the procedure based on similarity transformation for solving the matrix eigenproblem in multigroup calculations is time consuming and, moreover, the computational cost increases rapidly as the matrix order increases. In calculating a nine-group fast breeder reactor problem, the CPU time ratio can be as large as 2.4 : 1. In a certain sense, the increased computing times reflect the algebraic complexity of the analytic nodal method in multigroup calculations.

Table 4 Summary of results for the four-group MOX-fueled core problem

Method	Meshes/Assembly	k_{eff}[a)]	$E_{\max}$ (%)	E_{rms} (%)	CPU (s)
Analytic method	1×1	1.067562	0.28	0.18	0.08
Semi-analytic method		1.067521	0.30	0.19	0.06
Analytic method	2×2	1.067371	0.10	0.07	0.19
Semi-analytic method		1.067383	0.10	0.07	0.15

[a)] Reference: 1.067277

5. Four-Group KOEBERG Test Problem

The four-group KOEBERG test problem[20)] is a two-dimensional PWR problem with realistic cross section data including general up- and down-scattering. The problem is a model of an actual operating reactor core that consists of fuel assemblies with three different enrichments and three different burnable absorber loadings. Each fuel assembly is 21.608 cm wide. The core is surrounded by a homogenized reflector with vacuum boundary conditions. The reference solution was obtained with sixth-order matrix response method LABAN-PEL calculation.[20)] While more than 2% maximum errors (shown in **Table 5**) are observed in both analytic and semi-analytic nodal calculations using an assembly-size mesh, remarkable improvements are obtained by using 10.804 cm mesh (4 meshes per assembly). With the assembly-size mesh, the semi-analytic result is slightly more accurate than the analytic nodal result.

6. Modified Two-Dimensional IAEA Benchmark Problem

To verify the stabilization technique for the analytic nodal method, we modified the two-dimensional IAEA problem so that near singularity occurs in the three assemblies indicated by fuel type 5 as shown in **Fig. 3** (shaded areas). By increasing the thermal absorption cross sections from 0.085 cm^{-1} to 0.087277 cm^{-1} in the three assemblies, small eigenvalues of order 1.0×10^{-7} will appear for the buckling matrices during the analytic nodal calculations. The problem was calculated in single-precision arithmetic by using both the proposed and conventional analytic nodal methods. In the latter method, the two-node solution method is based on Eq. (50) and approximations are made in both homogeneous and particular solutions in case of near singularity. By contrast the proposed method only makes approximation to the particular solution. If the condition $|\lambda_j|_{\min}<\varepsilon$ is satisfied in a node, stabilization techniques are activated there. Various criteria of near singularity were used to test the performance of the methods. The results in **Tables 6** and **7** are compared with the reference solution obtained by using the semi-analytic nodal method and fine mesh (16 meshes per assembly). Because of the near singular assemblies, both calculations diverge in the first cases when no stabilization technique is used. When the criterion $\varepsilon=10^{-4}$ is used in the second cases to activate the stabilization techniques for the near singular nodes, both calculations converge to nearly the same result. As the criteria are relaxed and therefore more and more nodes, many of which are actually far from singularity, are treated as near singular node, the errors due to the approximations made in the stabilization technique also increase. However the proposed method is more robust than the conventional method. For example, the buckling matrix of assembly type 2 has an eigenvalue of order 5.0×10^{-4}. When the stabilization techniques are activated for the assembly type 2 in the third cases, the result of the proposed method is still quite accurate, whereas the result of the conventional method is totally unacceptable. The results indicate that the error due to the linear approximation to the homogeneous solution is relatively sensitive to the criterion of near singularity and a tighter criterion should be used for the conventional method. The analysis of a modified KOEBERG problem has also confirmed this result. It is found that the criterion $\varepsilon=10^{-4}$ is appropriate for the proposed method.

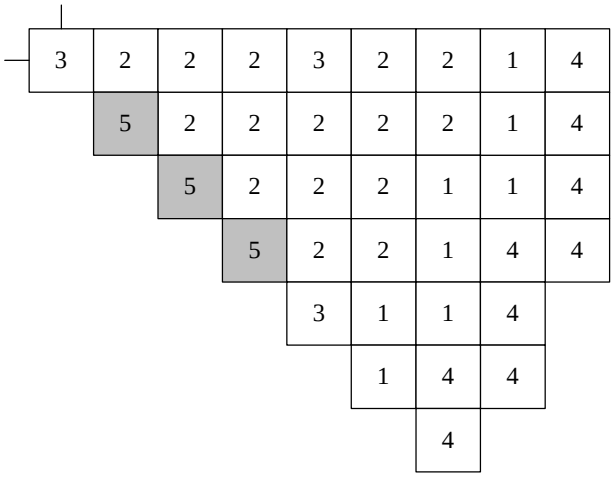

Fig. 3 The octant configuration of modified two-dimensional IAEA problem

IV. Conclusions

Two nonlinear nodal methods for solving the multigroup neutron diffusion equations have been presented and numerically evaluated. Based on the analytic and semi-analytic methods, the relationships between the surface flux and current were derived, which can provide efficient formulations for the two-node problem to be solved in the nonlinear iteration. The complex eigenmodes and instability problem inherent in the analytic solution were treated so that the algorithm is efficient as well as stable. The accuracy of the stabilized analytic nodal method was proven to be less sensitive to the criterion of near singularity. The two nodal methods were shown to be of about the same accuracy in the benchmarking calculations. Because of the transcendental components contained

Table 5 Summary of results for the four-group KOEBERG test problem

Method	Meshes/Assembly	k_{eff} [a)]	$E_{\max}$ (%)	E_{rms} (%)	CPU (s)
Analytic method	1×1	1.008386	2.22	1.27	0.24
Semi-analytic method		1.008356	2.08	1.17	0.18
Analytic method	2×2	1.007999	0.21	0.11	0.56
Semi-analytic method		1.007999	0.21	0.11	0.42

a) Reference: 1.007954

Table 6 Performance of the proposed method with various criteria of near singularity

Criterion ε	Singular assembly types	Number of nodes treated as singular[a)]	k_{eff} [b)]	$E_{\max}$ (%)	E_{rms} (%)
1.0×10^{-8}	No	0	Diverges	Diverges	Diverges
1.0×10^{-4}	5	3	1.026708	0.90	0.30
5.0×10^{-4}	5, 2	33	1.026773	0.95	0.32
2.0×10^{-3}	5, 2, 1	48	1.026955	8.83	2.79
5.0×10^{-2}	5, 2, 1, 3, 4	69	1.025754	7.60	2.68

a) Total number of nodes: 69 (quarter core)
b) Reference: 1.026619

Table 7 Performance of the conventional method with various criteria of near singularity

Criterion ε	Singular assembly types	Number of nodes treated as singular[a)]	k_{eff} [b)]	$E_{\max}$ (%)	E_{rms} (%)
1.0×10^{-8}	No	0	Diverges	Diverges	Diverges
1.0×10^{-4}	5	3	1.026713	0.89	0.31
5.0×10^{-4}	5, 2	33	1.027756	5.16	2.20
2.0×10^{-3}	5, 2, 1	48	1.027238	8.52	4.03
5.0×10^{-2}	5, 2, 1, 3, 4	69	1.030429	27.6	9.48

a) Total number of nodes: 69 (quarter core)
b) Reference: 1.026619

in both methods, they are clearly more accurate than the polynomial scheme NEM, particularly when large flux gradients near the assembly interfaces are to be modeled as is the case with highly enriched MOX fuel assemblies. The relative efficiencies of the two methods depend on the number of the energy groups to be solved. For two-group problems, the analytic calculations are faster, however, the semi-analytic calculations are faster for multigroup problems. It appears that the semi-analytic method is a practical method for multigroup problems.

Acknowledgment

The authors are grateful to C. J. Park and K. W. Park of Korea Advanced Institute of Science and Technology for their help during the benchmarking.

References

1) M. R. Wagner, K. Koebke, "Progress in nodal reactor analysis," *Atomkernenergie*, **43**, 117 (1983).
2) R. D. Lawrence, "Progress in nodal methods for the solution of the neutron diffusion and transport equation," *Prog. Nucl. Energy*, **17**, 271 (1986).
3) K. S. Smith, "Nodal method storage reduction by nonlinear iteration," *Trans. Am. Nucl. Soc.*, **44**, 265 (1983).
4) T. M. Sutton, B. N. Aviles, "Diffusion theory methods for spatial kinetics calculations," *Prog. Nucl. Energy*, **30**, 119 (1996).
5) K. S. Smith, "An Analytic Nodal Method for Solving the Two-Group, Multidimensional, Static and Transient Neutron Diffusion Equations," Nucl. Engr. Thesis, Department of Nuclear Engineering, MIT, Cambridge, MA (1979).
6) J. M. Noh, N. Z. Cho, "A new approach of analytic basis function expansion to neutron diffusion nodal calculation," *Nucl. Sci. Eng.*, **116**, 165 (1994).
7) N. Z. Cho, Y. H. Kim, K. W. Park, "Extension of analytic function expansion nodal method to multigroup problems in hexagonal-z geometry," *Nucl. Sci. Eng.*, **126**, 35 (1997).
8) N. Z. Cho, C. J. Park, J. M. Noh, "Continued factoring approach for removal of numerical singularity in the transverse-integrated analytic nodal method," *Trans. Am. Nucl. Soc.*, **86**, 361 (2002).
9) H. G. Joo, G. Jiang, T. J. Downar, "Stabilization techniques for

the nonlinear analytic nodal method," *Nucl. Sci. Eng.*, **130**, 47 (1998).

10) R. A. Shober, "A nodal method for fast reactor analysis," *Proc. Computational Methods in Nuclear Engineering*, Williamsburg, VA, p. 3–33 (1979).
11) M. R. Wagner, "Three-dimensional nodal diffusion and transport theory methods for hexagonal-z geometry," *Nucl. Sci. Eng.*, **103**, 377 (1989).
12) H. L. Rajic, A. M. Ougouag, "ILLICO: A nodal neutron diffusion method for modern computer architectures," *Nucl. Sci. Eng.*, **103**, 392 (1989).
13) R. D. Lawrence, J. J. Dorning, "A nodal Green's function method for multidimensional neutron diffusion calculations," *Nucl. Sci. Eng.*, **76**, 218 (1980).
14) H. Finnemann, F. Bennewitz, M. R. Wagner, "Interface current techniques for multidimensional reactor calculations," *Atomkernenergie*, **30**, 123 (1977).
15) G. W. Stewart, *Introduction to Matrix Computations*, Academic Press, (1973).
16) J. C. Lefebvre, J. Mondot, J. P. West, *Benchmark Calculations of Power Distribution within Assemblies*, NEACRP-L-336, Organization for Economic Cooperation and Development, (1991).
17) D. R. Vondy, *et al.*, *VENTURE: A Code Block for Solving Multigroup Neutronic Problems Applying the Finite-difference Diffusion-theory Approximation to Neutron Transport—Version II*, ORNL-5062/R1, Oak Ridge National Laboratory, (1977).
18) *Benchmark Problem Book*, ANL-7416, Suppl. 2, Argonne National Laboratory, (1977).
19) J. M. Noh, N. Z. Cho, "A multigroup diffusion nodal scheme in rectangular and hexagonal geometries: Hybrid of AFEN and PEN methods," *Proc. Int. Conf. on the Physics of Reactors*, Mito, Japan, Vol. 1, p. A-50 (1996).
20) E. Z. Muller, Z. J. Weiss, "Benchmarking with the multigroup diffusion high-order response matrix method," *Ann. Nucl. Energy*, **18**, 535 (1991).